Published in final edited form as:
J Am Chem Soc. 2008 January 23; 130(3): 839–841.

A New Family of Multiferrocene Complexes with Enhanced Control of Structure and Stoichiometry via Coordination-Driven Self-Assembly and their Electrochemistry

Hai-Bo Yang[†], **Koushik Ghosh**[†], **Yue Zhao**[†], **Brian H. Northrop**[†], **Matthew M. Lyndon**[§], **David C. Muddiman**[§], **Henry S. White**[†], and **Peter J. Stang**[*,†]

†*Department of Chemistry, University of Utah, 315 South 1400 East, RM, 2020, Salt Lake City, Utah, 84112*

§*W. M. Keck FT-ICR Mass Spectrometry Laboratory and Department of Chemistry, North Carolina State University, Raleigh, North Carolina 27695*

Abstract

The design and synthesis of a new family of multiferrocene complexes with enhanced control of structure and stoichiometry via coordination-driven self-assembly is described. Insight into the structure and electronic properties of all supramolecules was obtained by electrochemical studies. The collective results provide an enhanced understanding of the influence of structural factors on the electrochemistry of multifunctional electroactive supramolecular architectures.

Molecules that exhibit multifunctionality, such as those with multiple electroactive or photoactive moieties, are of interest because of a variety of materials and synthetic applications. Ferrocene, for example, has been widely utilized in multifunctional compounds because it is a stable and readily oxidizable organometallic complex with the potential to be used in electroluminescent, information storage, and photochemical devices.[1] To date, most multifunctional ferrocenyl compounds have been prepared as, or incorporated into, polymers or dendrimers.[2] Typically synthesized using traditional covalent strategies, multifunctional polymers and dendrimers often require considerable synthetic effort and can be plagued by low yields and largely amorphous final structures. Molecular self-assembly processes offer considerable synthetic advantages including significantly fewer steps, fast and facile formation of final products, and specific, well-defined arrangements of individual components.

In the past two decades, coordination-driven self-assembly has evolved to be a well-established process for the preparation of nanoscopic supramolecular ensembles with predetermined shapes, sizes, and geometries.[3] Stimulated by the power and versatility of this paradigm, we envisioned that functionalization of a *bis*pyridyl donor unit (Figure 1) would, when combined with an appropriately designed Pt(II) acceptors, lead to the formation of a new family of multiferrocenyl rhomboidal and hexagonal structures. Moreover, this strategy allows for precise control over the shape and size of the resulting metallacycles as well as the distribution and total number of incorporated ferrocene moieties. This ability to fine-tune the size, shape, distribution, and distance between electroactive ferrocenes would help provide a greater understanding of the influence to electrochemistry caused by structural factors. This research also provides a new approach to the study of functional amplification[4], which is a property characteristic of living systems, but so far limited to dendrimers in synthetic systems.

stang@chem.utah.edu.

We have recently shown that the addition of functional groups, such as crown ethers and Fréchet-type dendrons,[5] at the vertex of 120° building units enables the preparation of novel, functionalized cavity-cored assemblies. Similarly, by attaching a ferrocene group on the periphery of a 120° donor building block it will, when combined with suitable 60°, 120°, or 180° acceptor units, give rise to rhomboidal or different sized hexagonal heterobimetallic systems. The ferrocenyl 120° donor precursor **1** can be easily prepared via a coupling reaction of ferrocene-1-carboxylic acid and 3,5-bis(pyridin-4-ylethynl)phenol. Stirring the mixture of **1** and 60°, 120°, or 180° di-Pt(II) acceptor **2**, **3**, or **4** in a 1:1 ratio respectively, resulted in the formation of the [2+2] rhomboid **5**, the [3+3] hexagon **6**, and the [6+6] hexagon **7** with pendant ferrocene groups at donor vertexes (Figure 2).

Multinuclear NMR (^{1}H and ^{31}P) analysis (Figure 3) of the reaction mixtures revealed the formation of discrete, highly symmetric species. The ^{31}P {^{1}H} NMR spectra of **5**–**7**, displayed a sharp singlet (ca. 12.2 ppm for **5,** 13.5 ppm for **6,** and −14.6 ppm for **7**) shifted upfield from the starting platinum acceptor **2**, **3**, and **4** by approximately 11.8 ppm, 6.0 ppm, and 8.3 ppm, respectively. This change, as well as the decrease in coupling of flanking ^{195}Pt satellites (ca. ΔJ = −197 Hz for **5**, ΔJ = −148 Hz for **6**, ΔJ = −79 Hz for **7**) is consistent with back-donation from the platinum atoms.Additionally, the protons of the pyridine rings exhibited downfield shifts (ca. α-H_{Py}, 0.22 −0.54 ppm; β-H_{Py}, 0.2 – 0.3 ppm), resulting from the loss of electron density upon coordination of the pyridine-N atom with the Pt(II) metal center.

ESI mass spectrometry provides further evidence for the formation of new multiferrocene systems. The ESI mass spectra for bisferrocenyl rhomboid **4** (Figure 2A) revealed a peak at *m/z* = 1609.2, corresponding to $[M - 2NO_3]^{2+}$. In the ESI-TOF mass spectra of **6** and **7** (Figure 2B and 2C), peaks at *m/z* = 2625.26 and *m/z* = 1743.81, attributable to $[M- 2\ OTf]^{2+}$ for **6** and $[M - 5\ OTf]^{5+}$ for **7** respectively, were observed as well. All peaks were isotopically resolved and they agree very well with the theoretical distribution. The collective analytical results indicate that the multiferrocenyl complexes can be easily prepared (>95%) through coordination self-assembly, thus avoiding the time-consuming procedures and low yields often encountered in covalent synthesis protocols.

Molecular force-field simulations were used to gain further insight into the structural characteristics of multiferrocene complexes **5**–**7** (Figure 2). A 1.0 ns molecular dynamics simulation (OPLS force field) was used to equilibrate supramolecules **5**–**7**, followed by energy minimization of the resulting structures to full convergence. The model structure of bisferrocenyl rhomboid **4** features a well-defined rhombus with an approximate 2.4×1.6 nm cavity. Likewise, simulations revealed very similar planar hexagonal structures for trisferrocenyl hexagon **6** and hexaferrocenyl hexagon **7**, yet different sized cavities (3.3×3.1 nm for **6**, 5.3×5.1 nm for **7**).

Cyclic voltammetric measurements of ferrocenyl donor **1** as well as multiferrocene complexes **5**–**7** were performed in a dichloromethane solution containing 0.1M *n*-Bu_4NPF_6 as the supporting electrolyte using a platinum electrode.[6] The cyclic voltammograms corresponding to the 1-*e* electron oxidation of the ferrocene groups showed anodic/cathodic peak current ratios of $i_a/i_c \approx 1$ (Figure 4A, 4B). The half-wave potential, $E_{1/2}$, measured from the voltammetric waves are presented in Table 1. The potential difference between the anodic and cathodic peak potentials (ΔE_p) was found to be larger than the theoretical value of 59mV expected for a reversible 1-e redox reaction at the scan rates surveyed,[7] a reflection of ohmic resistance in the solution.[8]

To gain additional insight into the structure and electronic properties of **5**–**7,** potential-step chronoamperometry was performed to directly determine the diffusion coefficient, *D,* for each compound using microdisk electrodes without knowing the number of reaction sites, θ_{sites}, and

the redox concentration.[9] In the chronoamerometry experiment, the current i(t) was monitored as a function of time and normalized with respective to the steady state current $i_{lim.}$. When the electron transfer (ET) reaction initially happens, a concentration gradient is created and results in a continuing flux of redox molecules to the electrode surface. As ET continues to occur, the slope of the concentration profile at the electrode surface declines with time, as does the current. A plot of i(t)/ i_{lim} vs $t^{-1/2}$ showed, with increasing time, a linear response and diffusion coefficient D can be directly determined[10] from the slope of this linear relationship (See Supporting Information for details). The results are reported in Table 1. The ratio of the diffusion coefficients of rhomboid **5,** triferrocenyl hexagon **6** and hexaferrocenyl hexagon **7** is 3.0: 1.8:1.0, indicating that their hydrodynamic diameters lie in the inverse ratio of 1:1.7:3.0, since D is inversely proportional to the molecular size. Molecular force field simulations showed outer diameters of about 3.0, 4.2 and 6.9 nm for **5**, **6** and **7**, respectively, which are in relative, qualitative agreement with the experimentally determined ratio (Figure 2).

It is of interest to investigate the number of the electroactive sites for compounds **5**–**7**, which have 2, 3 and 6 ferrocenyl groups, respectively, attached to the metallacycles. The steady-state limiting current obtained from disk electrodes of known sizes (Figure 4), along with diffusion coefficients determined from chronoamperometry, could be used to calculate θ_{sites} using equation $i_{lim}=4nFDaC\theta_{sites}$ (1), where n is the number of electrons transferred per ferrocenyl site, F is the Faraday constant, C is the bulk concentration, θ_{sites} is the average number of reactive Fc sites per molecule, and a is the radius of the electrode.[11]

Considering the absence of strong intramolecular electronic coupling bridges between the ferrocenes in the structures of assemblies **5**–**7**, one-electron reactions are expected to be observed when analyzing the waveshape of steady state voltammograms plotted as $\log[(i_{lim}-i)/i]$ versus E.[12] The calculated slopes of **5**, **6**, and **7** are 52 mV, 56 mV and 54 mV, which are near the ideal value (0.059/n with n = 1) indicating that the redox species react one-at-a-time, more or less independently of one another. Calculated θ_{sites} from equation (1) match well for compounds **5**–**7** with site numbers of roughly 2, 3, and 6. (Table 1), demonstrating all the ferrocenyl groups attached to the metallacycles are electroactive.

In conclusion, we present a facile and versatile strategy for the synthesis of multiferrocenyl complexes where coordination-driven self-assembly allows precise control over metallacycle shape and size and the distribution of ferrocene moieties. Electrochemical studies reveal that all of the redox sites attached to complexes **5**–**7** are stable, independent, electrochemically active, and display 2, 3, and 6 reaction sites, respectively. All heterobimetallic compounds show one-electron reaction responses, with the additional electroactive sites enhancing the magnitude of current. Furthermore, the increased size of the assemblies also results in a decrease in the diffusion coefficient, D. These findings provide an enhanced understanding of the influence of structural factors on the electrochemistry of multifunctional electroactive supramolecular metallacycles and make them of interest as potential multi electron redox catalysis, electron reservoirs, electrode modifiers, ion-sensors and mimics of biological redox process that are easily self-assembled.

Supplementary Material

Refer to Web version on PubMed Central for supplementary material.

Acknowledgements

P.J.S. thanks the NIH (GM-057052) and the NSF (CHE-0306720) for financial support. B.H.N. thanks the NIH (GM-080820) for financial support. H.S.W. thanks the NSF for financial support. D.C.M. and M.M.L. thank NCBC and NCSU for generous financial support.

References

1. (a) Sun S-S, Lees AJ. Inorg Chem 2001;40:3154. [PubMed: 11399187] (b) van Staveren DR, Metzler-Nolte N. Chem Rev 2004;104:5931. [PubMed: 15584693] (c) You C-C, Wurthner F. J Am Chem Soc 2003;125:9716. [PubMed: 12904037] (d) Shoji O, Okada S, Satake A, Kobuke Y. J Am Chem Soc 2005;127:2201. [PubMed: 15713098] (e) Das N, Arif AM, Stang PJ, Sieger M, Sarkar B, Kaim W, Fiedler J. Inorg Chem 2005;44:5798. [PubMed: 16060632] (f) Chebny VJ, Dhar D, Lindeman SV, Rathore R. Org Lett 2006;8:5041. [PubMed: 17048838] (g) Mereacre V, Nakano M, Gomez-Segura J, Imaz I, Sporer C, Wurst K, Veciana J, Turta C, Ruiz-Molina D, Jaitner P. Inorg Chem 2006;45:10443. [PubMed: 17173397] (h) Collinson MM. Acc Chem Res 2007;40:777. [PubMed: 17458928] (i) Lang H, Packheiser R. Collect Czech Chem Commun 2007;72:435.
2. (a) Fréchet JM. Science 1994;263:1710. [PubMed: 8134834] (b) Rulkens R, Lough AJ, Manners I, Lovelace SR, Grant C, Geiger WE. J Am Chem Soc 1996;118:12683. (c) Valerio C, Fillaut J-L, Ruiz J, Guittard J, Blais J-C, Astruc D. J Am Chem Soc 1997;119:2588. (d) Castro R, Cuadrado I, Alonso B, Casado CM, Moran M, Kaifer AE. J Am Chem Soc 1997;119:5760. (e) Anicet N, Anne A, Moiroux J, Savéant J-M. J Am Chem Soc 1998;120:7115. (e) Nlate S, Ruiz J, Blais J-C, Astruc D. 2000:417. (f) Nguyen P, Gomez-Elipe P, Manners I. Chem Rev 1999;99:1515. [PubMed: 11849001] (g) Brinke G, Ikkala O. Science 2002;295:2407. [PubMed: 11923526] (h) Stone DL, Smith DK, McGrail PT. J Am Chem Soc 2002;124:856. [PubMed: 11817961] (i) Choi T–L, Lee K-H, Joo W-J, Lee S, Lee T-W, Chae MY. J Am Chem Soc 2007;129:9842. [PubMed: 17645335]
3. (a) Stang PJ, Olenyuk B. Acc Chem Res 1997;30:502. (b) Leininger S, Olenyuk B, Stang PJ. Chem Rev 2000;100:853. [PubMed: 11749254] (c) Seidel SR, Stang PJ. Acc Chem Res 2002;35:972. [PubMed: 12437322] (d) Schwab PFH, Levin MD, Michl J. Chem Rev 1999;99:1863. [PubMed: 11849014] (e) Holliday BJ, Mirkin CA. Angew Chem Int Ed 2001;40:2022. (f) Cotton FA, Lin C, Murillo CA. Acc Chem Res 2001;34:759. [PubMed: 11601960] (g) Fujita M, Tominaga M, Hori A, Therrien B. Acc Chem Res 2005;38:369. [PubMed: 15835883] (h) Fiedler D, Leung DH, Bergman RG, Raymond KN. Acc Chem Res 2005;38:349. [PubMed: 15835881]
4. (a) Groot de FMH, Albrecht C, Koekkoek R, Beusker PH, Scheeren HW. Angew Chem Int Edn Engl 2003;42:4490. (b) Amir RJ, Pessah N, Shamis M, Shabat D. Angew Chem Int Edn Engl 2003;42:4494. (c) Li S, Szalai ML, Kevwitch RM, McGrath DV. J Am Chem Soc 2003;125:10516. [PubMed: 12940723]
5. (a) Yang H-B, Das N, Huang F, Hawkridge AM, Muddiman DC, Stang PJ. J Am Chem Soc 2006;128:10014. [PubMed: 16881621] (b) Yang H-B, Hawkridge AM, Huang SD, Das N, Bunge SD, Muddiman DC, Stang PJ. J Am Chem Soc 2007;129:2120. [PubMed: 17256935] (c) Yang H-B, Ghosh K, Northrop BH, Zheng Y-R, Lyndon MM, Muddiman DC, Stang PJ. J Am Chem Soc. 2007in press
6. The complexes remain unchanged before and after the cyclic voltametry measurement as indicated by NMR analysis.
7. Matsuda H, Ayabe Y. Z Electrochem 1955;59:494.
8. It is not uncommon for the resistance to be in the range of several kΩ even with 0.1 M supporting electrolyte.
9. (a) Denault G, Mirkin M, Bard AJ. J Electroanal Chem 1991;308:27. (b) Biondi C, Bellugi L. J Electroanal Chem 1970;24:263. (c) Amatore C, Azzali m, Calas P, Jutand A, Lefrou C, Rollin Y. J Electroanal Chem 1990;288:45. (d) Mirkin MV, Nilov AP. J Electroanal Chem 1990;283:35. (e) Nowinski SA, Anjo DM. J Chem Eng Data 1989;34:265.
10. (a) Jaworski, Al; Donten, M.; Stojek, ZJ. J Electroanal Chem 1996;407:75. (b) Paulse CD, Pickup PG. J Phys Chem 1988;92:7002.
11. Bard, AJ.; Faulkener, LR. Electrochemical Methods: Fundamentals and Applications. Wiley, New York: Wiley; p. c1980
12. (a) Miles DT, Murray RW. Anal Chem 2001;73:921. [PubMed: 11289437] (b) Templeton AC, Cliffel DE, Murray RW. J Am Chem Soc 1999;121:7081.

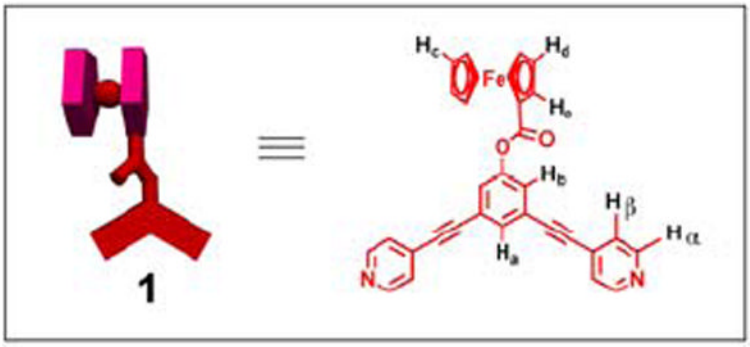

Figure 1.
Schematic, molecular, and X-ray structure of ferrocenyl donor **1**.

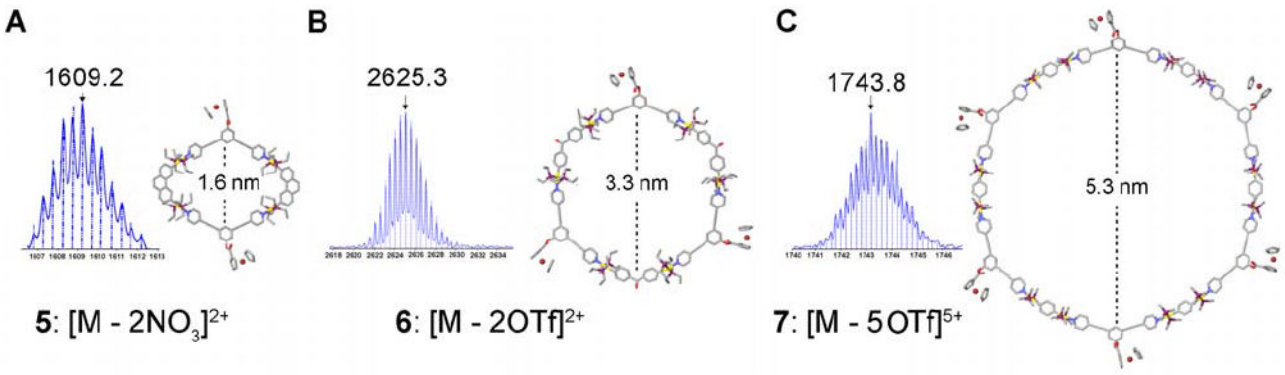

Figure 2.

ESI-MS spectra and molecular force field model of bisferrocenyl rhomboid **5** (**A**). ESI-TOF-MS spectra and molecular force field models of trisferrocenyl hexagon **6** (**B**) and hexakisferrocenyl hexagon **7** (**C**). For each spectra vertical lines indicate the theoretical abundances while the solid line is the experimental result.

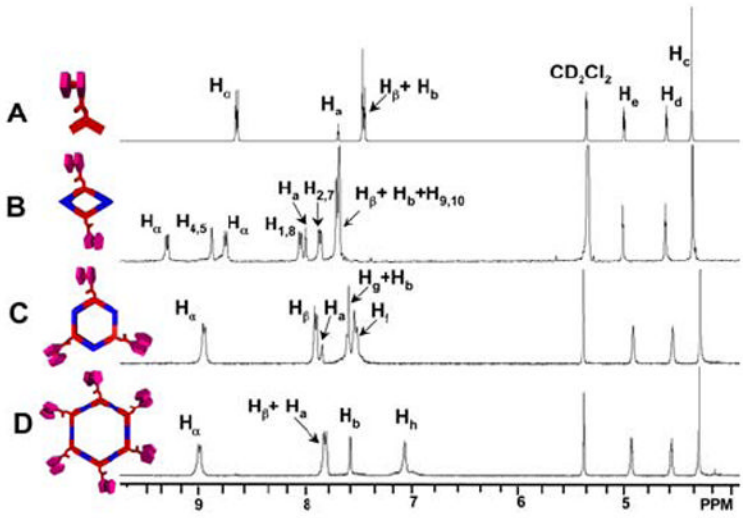

Figure 3.
Partial ^{1}H NMR spectra recorded at 500 MHz (CD_2Cl_2, 298 K) of donor **1** (A), rhomboid **5** (B), and hexagons **6** (C) and **7** (D).

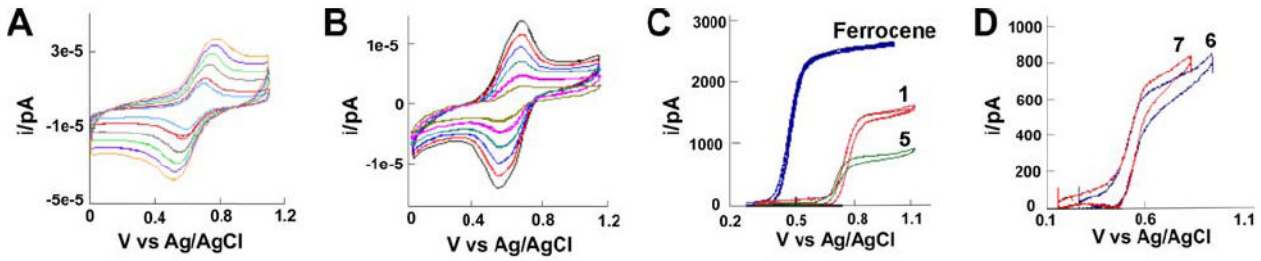

Figure 4.

Cyclic Voltammograms of 0.20 mM **6** (**A**) and 0.21mM **7** (**B**) at a scan rate of 25-250 mV/s. Steady-State response on a Pt ultramicroelectrode at a scan rate of 20mV/s for 0.22mM Fc, 0.20mM 1, 5, 6 and 0.21mM 7 (**C**, **D**) in CH_2Cl_2 containing 0.1M *n*-Bu_4NPF_6.

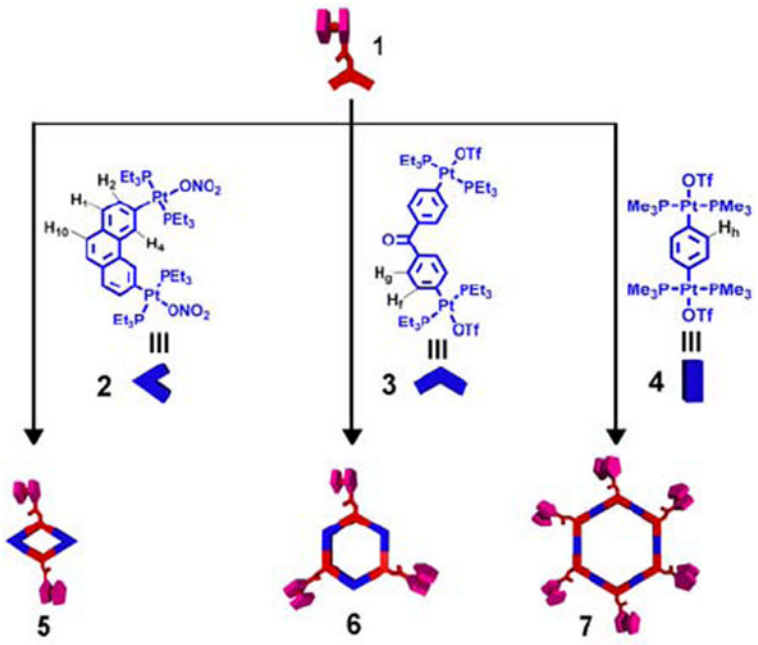

Scheme 1.

Molecular structures of **2** – **4**, as well as a graphical representation of the self-assembly of heterobimetallic compounds **5** – **7**.

Table 1

Results of electrochemical (CH_2Cl_2 with 0.1 M *n*-Bu_4NPF_6, 298 K) studies of free ferrocene and multiferrocenyl compounds **5**-**7**.

Compound	$E_{1/2}$ (V vs Ag/AgCl)	$10^6 D$ ($cm^2 \cdot s^{-1}$)	θ_{sites}
Ferrocene	0.479± 0.004	18.1 ± 1.18	1.2±0.078
1	0.802± 0.004	8.78 ± 0.206	1.1±0.026
5	0.765± 0.002	2.16 ± 0.208	2.0±0.19
6	0.652± 0.003	1.40 ± 0.150	2.9±0.31
7	0.644± 0.007	0.816 ± 0.0330	5.8±0.24